RUSSIAN JOURNAL OF EARTH SCIENCES, VOL. 7, NO. 1, PAGES 1–19, FEBRUARY 2005

Paleomagnetism of rocks in the Phanerozoic Terrains of southeast Russia: Comparison with data for the North China Platform: A review

Yu. S. Bretshtein and A. V. Klimova

Institute of Tectonics and Geophysics, Far East Division, Russian Academy of Sciences

Abstract. This paper presents the results obtained by the authors in the last years during their paleomagnetic studies of the Paleozoic and Mesozoic rocks in the Sikhote-Alin and Mongolia-Okhotsk superterrains, and also of the terrains attributed to the Amur Plate. These results are compared with the paleomagnetic data available for the North China and Siberian Cratons. Being similar to one another in many respects, the APWPs for the Sikhote-Alin and Mongolia-Okhotsk superterrains and for the North China Craton grew substantially different from the APWP for the Siberian Craton, reflecting the divergence of the terrains of the Mongolia-Okhotsk and Sikhote-Alin foldbelts, similar to the divergence of the North China Plate and the Siberian Craton. A significant role is demonstrated for the remagnetization of the rocks during the Mesozoic in the course of accretion-collision folding.

Introduction

The area of the mullion articulation of the differently oriented Mongolia-Okhotsk (MO) and Sikhote-Alin (SA) foldbelts, as well as the collision zones between the Siberian and North China cratons, is known for the wide development of geologically different structural facies zones (terrains), which are combined by some geologists into the Amur Plate [*Zonenshain et al.,* 1990]. They produce an intricate mosaic of geologic blocks, the tectonic positions of which cannot be interpreted without using the views of terrains and their close associations in the past with the genetically similar geologic objects proved in the neighboring territories of China, Korea, and Mongolia. The "independence" of these structural features or their belonging to the China and/or to the Siberian cratons is a subject of many discussions. It appears that this region is a key object for the study and interpretation of the tectonic history of the interaction of these geoblocks at the junction of the Siberian, Pacific, and North China plates.

Paper number TJE04168.
ISSN: 1681–1208 (online)

The online version of this paper was published 18 March 2005.
URL: http://rjes.wdcb.ru/v07/tje04168/tje04168.htm

In spite of the general growth of interest in the study of the geologic history of the region in terms of plate tectonics, paleomagnetic studies were carried out there, until recently, in a sporadic manner. Almost until the middle of the 1990s the single publications dealing with the rocks older than Meso-Cenozoic (Permian-Mesozoic) with references to paleomagnetic data were mainly reviews for the Pacific region as a whole [*Ustritskii and Khramov,* 1987]. The authors of some papers reported results that did not satisfy the criteria of estimating the reliability of paleomagnetic data collections (the low quality of laboratory magnetic cleaning, the lack of the component analysis of the results of NRM demagnetization, and of the evidence for the use of various tests for detecting NRM ancient and primary components) [*Zakharov and Sokarev,* 1991]. The rocks that can be ranked at the present time as relatively well studied are only the Mesozoic and Cenozoic rocks of the Primorie and Priamurie regions [*Bretshtein,* 1988, 1991; *Klimova and Bretshtein,* 1993; *Otofuji Yo-ichiro et al.,* 1995]. It was only recently the paleomagnetic studies were carried out in some areas of SE Russia, which provided the first paleomagnetic data for the Paleozoic and Mesozoic terrigenous and carbonate rocks of the Primorie, Priamurie, and East Baikal regions [*Bazhenov et al.,* 1999; *Bretshtein et al.,* 1999; *Bretshtein et al.,* 2003; *Kurilenko et al.,* 2001].

It should be noted that some negative circumstances complicated significantly the correlation and interpretation of paleomagnetic data, especially because of the wide develop-

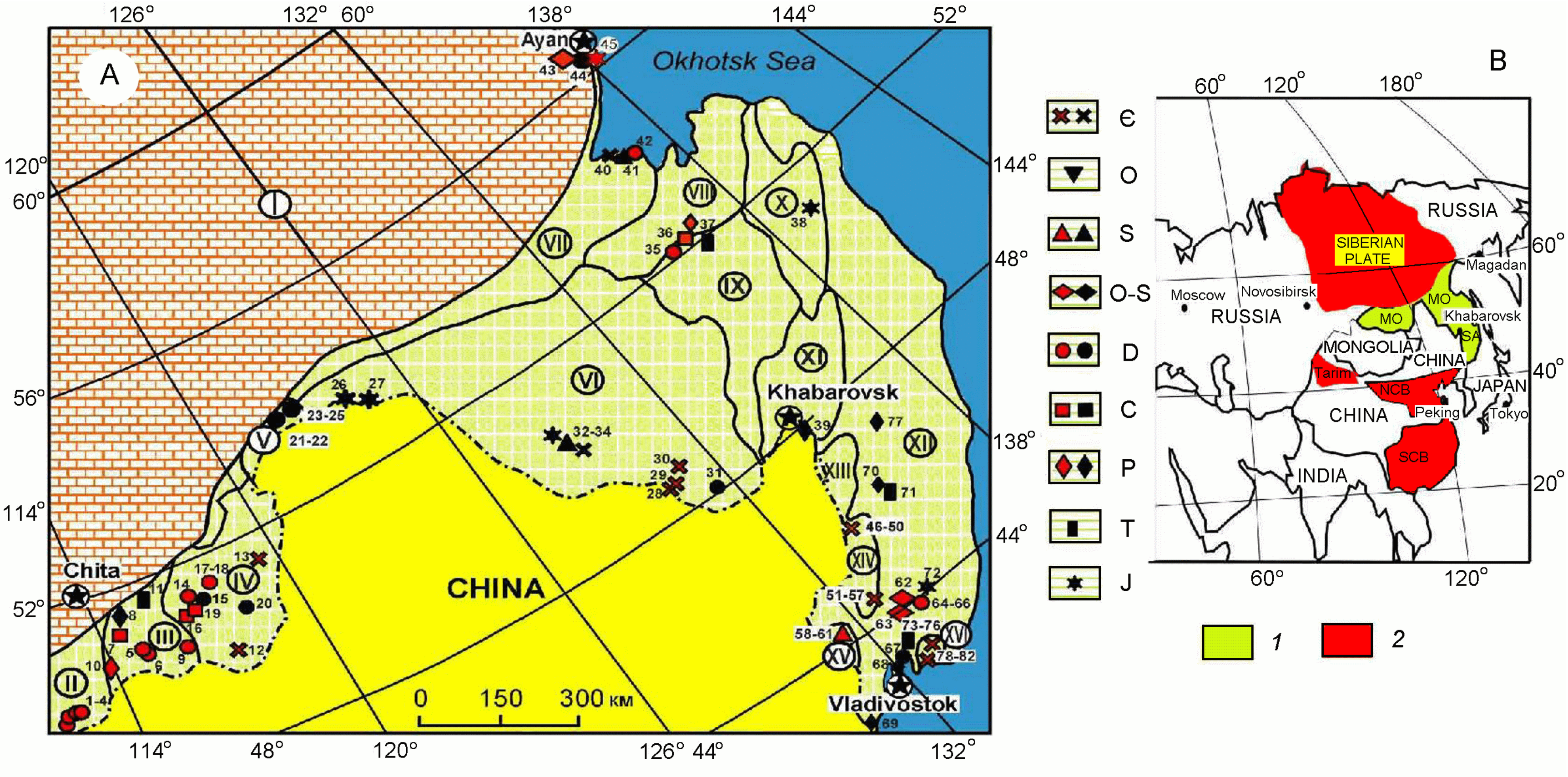

Figure 1. Schematic location map showing the paleomagnetic knowledge of the Phanerozoic sedimentary-metamorphic rocks in the main geostructural units in the south of the Russian Far East territory. (A): (I) Siberian Platform; terrains: (II) Khentay-Dauria, (III) Aga, (IV) Argun, (V) Oldoi, (VI) Khingan-Bureya, (VII) Tukuringra-Dzhagda, Gonzha, Mamyn, Ayan-Shevla, and Galama (Mongolia-Okhotsk superterrain), (VIII) Ulba and Kerba, (IX) Badzhal, (X) Kiselev-Manoma, (XI) Khabarovsk, (XII) Sikhote-Alin accreted subterrain and the Sinegorsk zone of collision-related terrains, (XIII) Nakhimov, (XIV) Spassk, (XV) Laolin-Grodekovo, and (XVI) Sergeevka terrain. Shown by symbols are the main areas of study and the geological ages of the rocks (the numbers of the study areas correspond to those of the areas listed in the Table 1). The red (or black) symbols show the rock sequences where prefolding magnetization was preserved (or not preserved, or is problematic). The age symbols are (E) Vendian-Cambrian, (O) Ordovician, (S) Silurian, (D) Devonian, (C) Carboniferous, (P) Permian, (T) Triassic, and (J) Jurassic. (B): The mutual positions of the plates and of the foldbelts studied in the Asia-Pacific continental margin. 1 – The composite terranes of the "Amurian plate" enclosing Mongol-Okhotsk (MO) and Sikhote-Alin (SA) fold belts; 2 – the main "rigid" plates (blocks; NCB (SCB) are the North (South) China block.

ment of remagnetized rocks, and also because of the insufficiently exact dating of the rock sequences, in many cases with an accuracy of a series, and most commonly, to a period. The isotopic ages of many igneous rocks were interpreted ambiguously because of a great data scatter. The fauna-based dating of sedimentary rocks admitted, in some cases, the wide age range of their accumulation, during which numerous tectonic events might have occurred, contributing to the remagnetization of the rocks. Many fossil-bearing and magnetically stable rocks could not be used because they belonged to the unstratified matrix in the form of blocks or olistostromes. The substantial amounts of rocks turned out to be almost nonmagnetic (their magnetization was measured at the sensitivity limit of the modern instruments). For this reason, about half of the collected and processed samples were discarded.

Finally, still urgent is the problem of the comparability of paleomagnetic data, namely, of the paleopole positions for the foldbelt terrains of the Far East Region of Russia, as well as for the Siberian and North China plates. As will be demonstrated below, the Paleozoic paleomagnetic data available for the latter are based on the scarce and often fairly contradictory data obtained for the North China and Korea (with the accuracy of the age gradation comparable with that used in our study). The age "sliding" to some or other side is possible for both regions.

In spite of the sufficiently large volume of laboratory magnetic cleanings and the use of modern data processing techniques, the above-mentioned circumstances predetermined the preliminary character of many of the resulting data. The paleomagnetic data should permanently added, analyzed, periodically revised, and constantly revised.

Below we reported the results of the recent paleomagnetic investigations of the terrigenous rock investigated by the authors in the Sikhote-Alin and Mongolia-Okhotsk superterrains and also in the terrains attributed to the Amur platform (Figure 1).

Methods of Paleomagnetic Studies

The laboratory measurements and experimental studies were carried out using modern cryogenic magnetometers, rock generators (spinner magnetometers), and various demagnetizing devices in Russian and foreign laboratories: at the Institute of Tectonics and Geophysics, Far East Division, Russian Academy of Sciences (RAS), at the Geological Institute (RAS), at the Institute of Physics of the Earth (RAS), at the Institute of Geology and Geophysics, Siberian RAS Division, at Far-East Geological Survey, at the "Borok" Geophysical Observatory of the Institute of Physics of the Earth (RAS), at the Institute of Geophysics, Ukrainian Academy of Sciences, at the Institute of Tectonics, Californian University, and at the Montpellier-2 University, France. These studies included all modern experimental methods, including stepwise thermal demagnetization at temperatures up to 690°C and AF demagnetization up to 100 mT. NRM carriers were investigated to determine various magnetic mineral characteristics, this allowing the estimation of the composition, structural state, and size of magnetic grains and their quantitative relationships in the samples of the study rocks. These characteristics were the coercive force H_c, the value and temperature control of saturation magnetization J_s, of remanent saturation magnetization I_{rs} and of magnetic susceptibility χ, and the variation of isothermal remanent magnetization as a function of the permanent field of its creation $J_{\mathrm{r}}(H)$.

The paleomagnetic data were processed using modern statistical (analytical and graphical) methods using a component analysis [*Kirschvink,* 1980; *Zijderveld,* 1967], remagnetization circle remagnetization [*Halls,* 1978; *Khramov et al.,* 1982], including the separation of a sector for estimating the mean direction [*McFadden and McElhinny,* 1988], various fold test modifications [*McFadden,* 1990; *McFadden and Jones,* 1981; *Shipunov,* 1995a; *Shipunov and Muraviev,* 2000; *Watson and Enkin,* 1993], a reversal test [*McFadden and McElhinny,* 1990; et al.], conglomerate and burning tests, as well as various methods for isolating pre-, syn-, and post-folding NRM components [*Shipunov,* 1995b; *Shipunov and Bretshtein,* 1999]. The computer data processing was performed using the Enkin, McFadden, and Shipunov programs.

Figure 2 shows the curves characterizing the ferromagnetic minerals responsible for the magnetization of the study rocks. The main magnetization carriers of the rocks are magnetite, hematite, and pyrrhotite, as can be seen from the blocking temperatures (Curie points), the latter being usually responsible for the relatively low-temperature magnetization, caused by the secondary superposed processes operating in the course of folding, namely by heating and fluid flow. Hematite is represented (especially in the sandstone) by single and pseudodomain grains producing finely dispersed intergranular pigmentation. This mineral is also the carrier of syn- and pre-folding magnetization. The former is characteristic of the Silurian sandstones, investigated in the area of the Zeya R. middle flow. The Ordovician-Silurian silty sandstones of the Okhotsk (Ayan) area, the Cambrian rocks of the superposed Kimkan terrigenous-carbonate trough in the Amur region, and the Devonian silty sandstones in the Sinegorsk postcollision zone in Primorie, containing mostly hematite, preserved their prefolding high-temperature ChRM component. The most abundant mineral in the sedimentary rocks is magnetite; the concentration and size of its grains control the physical parameters and magnetic stability of many rocks in the region discussed.

The anisotropy of magnetic susceptibility (AMS) and of normal isothermal remanent magnetization (ASIRM) were studied for the purpose of estimating the potential effect of magnetic anisotropy on the distribution of the vectors of the characteristic ChRM component of natural remanent magnetization. Our analysis of the distribution of the rock magnetization vectors, as well as of the results of studying AMS using pilot objects, revealed an obvious correlation (coincidence or similarity) of the dips and strikes of the bedding planes and/or of the secondary schistosity, and also of the AMS and ASIRM planes of the sedimentary rocks with the average direction of the vector for the high-temperature ChRN component of NRM, often irrespective of the age, lithology, dips and strikes, and the tectonic conditions of

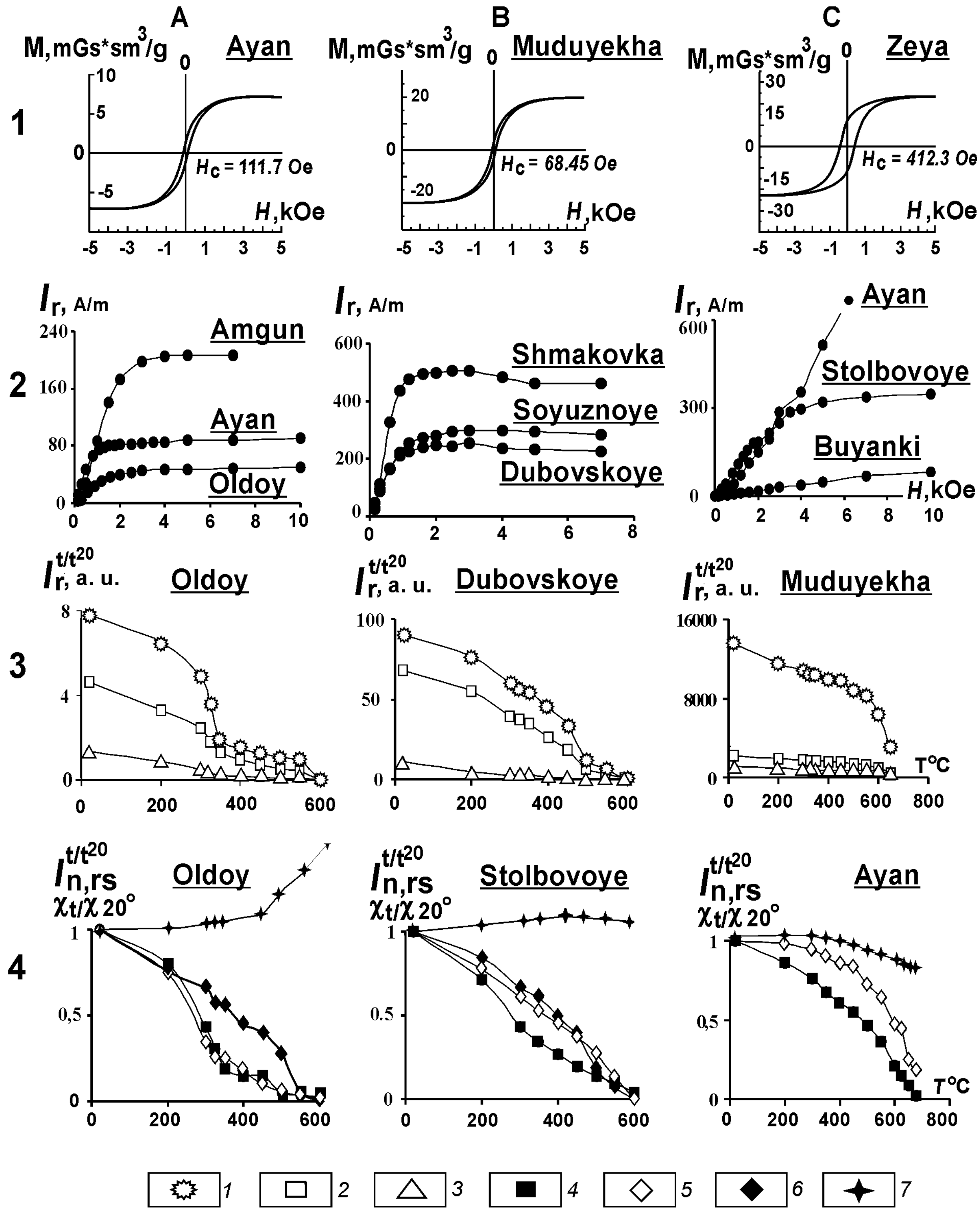

Figure 2. Characteristics of the ferrimagnetic minerals responsible for the magnetization of the rocks: (1) magnetic hysteresis loops, (2) curves of normal magnetization ($I_r(H)$ in kilooersteds, (3) $I_r(T)$ curves for different values of the H permanent magnetizing field directed along the X,Y, and Z axes of the rock samples [*Lowrie,* 1990], (4) normalized curves showing the temperature control of I_n, I_{rs}, and χ. The legend below the figure: (1) H = 10 kOe, (2) H = 0.05 kOe, (3) H = 0.01 kOe, (4) $I_n(T)$, (5–6) $I_{rs}(T)$ for the first and second heating, respectively, (7) $\chi(T)$. The minerals as magnetization carriers are (A) pyrrhotite, (B) magnetite, and (C) hematite.

the rock accumulation. This provided a basis for assuming, by analogy with other investigators [*Johns et al.,* 1997; *Tan and Kodama,* 2002], that the gently sloping ChRM vectors and the respective low paleolatitude values might have been caused not by the sediment deposition in the area of low paleolatidudes but by the lower inclination in the course of sediment packing and/or by the metamorphism during the subsequent folding, combined with the remagnetization of the rocks.

The regional remagnetization of the rocks and the "unexpectedly" gentle NRM inclinations (especially in the case of the Late Paleozoic and Mesozoic rocks) were reported earlier for many other regions of Southeast Asia [*Dobson and Heller,* 1992; *Kent et al.,* 1987; *Otofuji Yo-ichiro et al.,* 1989; *Wang and Van der Voo,* 1993; *Yang et al.,* 1989], yet, as a rule, they were treated as artifacts, without any detailed analysis of the mechanism that had caused them. On the whole this showed a fairly significant trend: compared to the rigid blocks of the platforms, the fold zones often show the flattening of the ChRM directions for the rocks varying from Cambrian to Triassic in age. Many of the Late Paleozoic and Early Mesozoic rocks of the foldbelts show the substantial "aging" of the paleopole position, compared to those of the platforms, or are distinguished by the "inadequate" directions of their characteristic NRM components, often with the predominant contribution of their synfolding and postfolding components and/or of their sums. It appears that this phenomenon is characteristic of all foldbelts of the world and can be a consequence of the postsedimentation packing of the sediments and/or of dislocation metamorphism in the course of orogeny during accretion-collision folding.

The paleomagnetic studies carried out for numerous objects of various Mongolia-Okhotsk and Sikhote-Alin terranes proved the wide distribution of this phenomenon. As an example illustrating this phenomenon, Figure 3 shows a number of parameters for the anisotropy of the Devonian rocks of the Oldoi Terrain. The presence of a relationship (correlation) between some of the AMS parameters and of the ChRM inclination value as a function of the K3/K1 anisotropy value, proved for some rock sequences, allows one to estimate the contribution of anisotropy to the lowering of inclination. The preliminary estimation of the amount of the potential deviation of the ChRM direction from the primary one (obtained after introducing corrections for anisotropy) was performed using a computer program written by V. N. Savoiskii. The value of this correction (dAMS) varies for different rock samples collected in the area discussed from a few to degrees to their first tens (see E in Figure 3). There are examples where the introduction of these corrections allowed some researchers to improve and even correct their conclusions about paleomagnetic directions, the paleolatitude positions of terrains, and the respective geodynamic conditions of the past. The examples can be found in [*Kim and Kodama,* 2004; *Raposo et al.,* 2003]. Since the detailed discussion of this problem is beyond the scope of this paper, we can merely note that in the case of some geological objects, where abnormally low paleomagnetic inclinations are observed, anisotropy may be responsible for them. In this case the fold test used in grouping rock sequences of the same age may be positive and may agree with the formal criteria used to identify a "prefolding" NRM component in the rock sequences examined, and the magnetic anisotropy value itself may be relatively low ($\sim$10%).

Figures 4 and 5 show the methods we used to distinguish stable high-temperature magnetization components and some results of our stepwise thermal demagnetization of some individual geological objects. The use of various paleomagnetic tests allowing one to date the formation of the magnetization of rock complexes at the level of geologic sections in individual terranes is demonstrated in Figure 6. The examples of the Vendian-Cambrian rocks of the Nakhimov and Spassk terrains and of the Permian-Carboniferous deposits of the Badzhal Terrain clearly show that these rocks preserved their prefolding magnetization. In other cases the rocks were remagnetized, which was confirmed by the respective tests after the grouping of the sections [*McFadden,* 1990; *Shipunov,* 1995a; *Watson and Enkin,* 1993]. A conglomerate test demonstrated the post-folding magnetization of the Ordovician-Silurian red magnetically stable, hematite-bearing sandstones of the Ayan-Shevli Terrain.

Review of the Paleomagnetic Results and Their Magnetotectonic Interpretation

The Table 1 presented at the end of this paper lists the tested paleomagnetic data characterizing the main Paleozoic and Mesozoic rock sequences which we studied in the areas of the Sea of Okhotsk coast, as well as in the areas of the Amur R. and in the area west of the Baikal Lake. After our temperature cleanings and test, only less than half of the studied rock sequences were found to be suitable for calculating the paleomagnetic pole. The objects which were used to calculate the positions of the paleopoles after their grouping are shown in Figure 7 are underlined in the Table 1. Proceeding from the accuracy of grading our age determinations and from the real statistical limits of the potential primary ChRM estimation from the wide spectrum of the NRM syn- and post-folding NRM components, we reckoned it to be expedient to average the paleomagnetic data in time using geological periods, thus avoiding some false detailing and, generally, reflecting more objectively the real pattern of the pole distribution for the present-day knowledge of the region.

Figure 7 shows the "evolution" of the views of various authors on the potential APWP trend for the North China Platform, based on the results obtained during the last 20 years. This figure also shows the results of our determinations for the Mongolia-Okhotsk (MO) and Sikhote-Alin (SA) superterranes, only part of them being published recently.

On the whole, the trends of the apparent drifting of the paleopole for the MO and SA terranes of the foldbelts and for the North China Platform were found to be almost parallel. The comparison of the various potential versions of these paths (controlled by the choice of the magnetization polarity of the rocks in Paleozoic time) showed their minimum "extension" when the SE-NW trend was chosen for the Cambrian-Carboniferous interval of time (see Figure 7

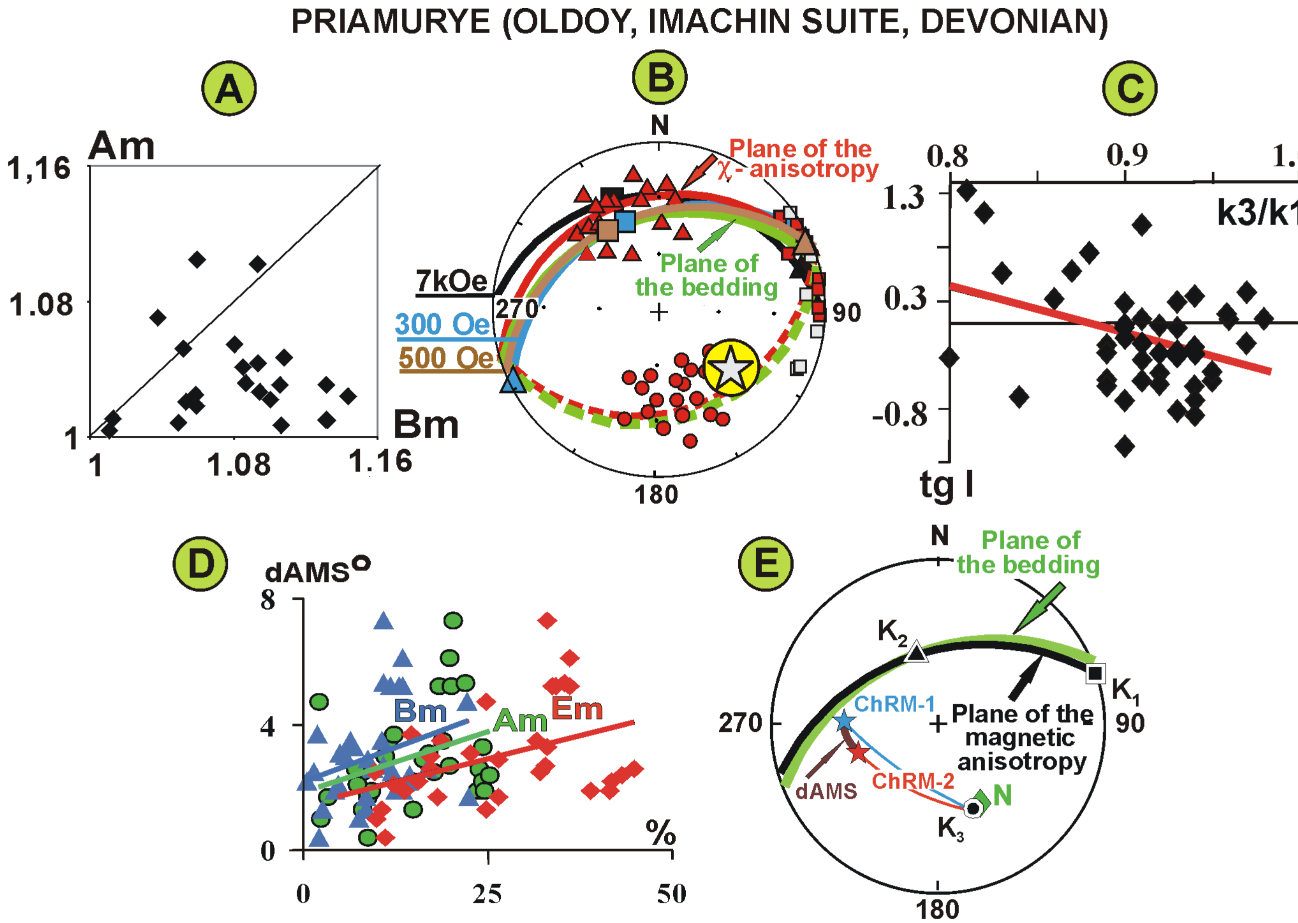

Figure 3. Relationships among the paleomagnetic, structural, and anisotropic characteristics. (A) Flinn diagram; (B) relations among the projections of the bedding plane (green), the axes and planes of the tensor ellipsoid of magnetic anisotropy susceptibility χ and IRM determined in the magnetic fields of 300, 500, and 7000 Oe with the ChRM direction (the asterisk denotes confidence values); the squares, triangles, and circles denote the large (K1), intermediate (K2), and small (K3) ellipsoid axes, respectively, the large symbols for K1 and K2, being their average directions for IRM; the solid light symbols and solid (or dash) lines show the projections of the axes and planes onto the lower (upper) hemisphere, respectively; the C curve shows the variation of inclination vector angles (tan I) in the ancient system of coordinates as a function of the anisotropy value (K3/K1), after [*Hodych et al.,* 1999]; D shows the variation of the ChRM inclination for anisotropy (dAMS) as a function of the Em, Am, and Bm parameters (%); E shows an example of the ChRM direction changes before (1) and after (2) introducing corrections for anisotropy, N being a normal to the bedding plane. B and E denote the modern system of the coordinates. The Oldoi Terrane (Amur R. area), Devonian silty sandstone.

(plate 6) for the details). In accordance with the principle of APWP minimization, we preferred direct polarity for the Lower-Middle Paleozoic using the SSW direction of the primary ChRM direction. In this version the MO and SA superterrains, as well as the North China Platform (NCP), are assumed to have been located at the nearly equatorial and subtropic latitudes of the Northern Hemisphere and, probably, in the northern periphery of East Gondwana. With the nearly paleolatitudinal position of the Mongolia-Okhotsk and Sikhote-Alin terranes, many of the independently drifting blocks, as follows from some differences in the position of the paleopole, might have experienced some local differentiated (often differently directed) rotations throughout the Paleozoic. Yet, on the whole, the general drifting trend of these geoblocks from the lower (nearly equatorial) to their present-day positions is fairly demonstrative.

The comparison of the most reliable paleomagnetic data, obtained for the foldbelt terrains of the Far-East territory of Russia, with the most correct results obtained for the North China Platform proved the proximity of their paleopole positions during the respective time interval. These results were obtained for some geographically close local rock sequences in the suture (fold) zones of the North China platform [*Gao et al.,* 1983; *He et al.,* 1988; *Huang et al.,* 1999, 2001; *Li*

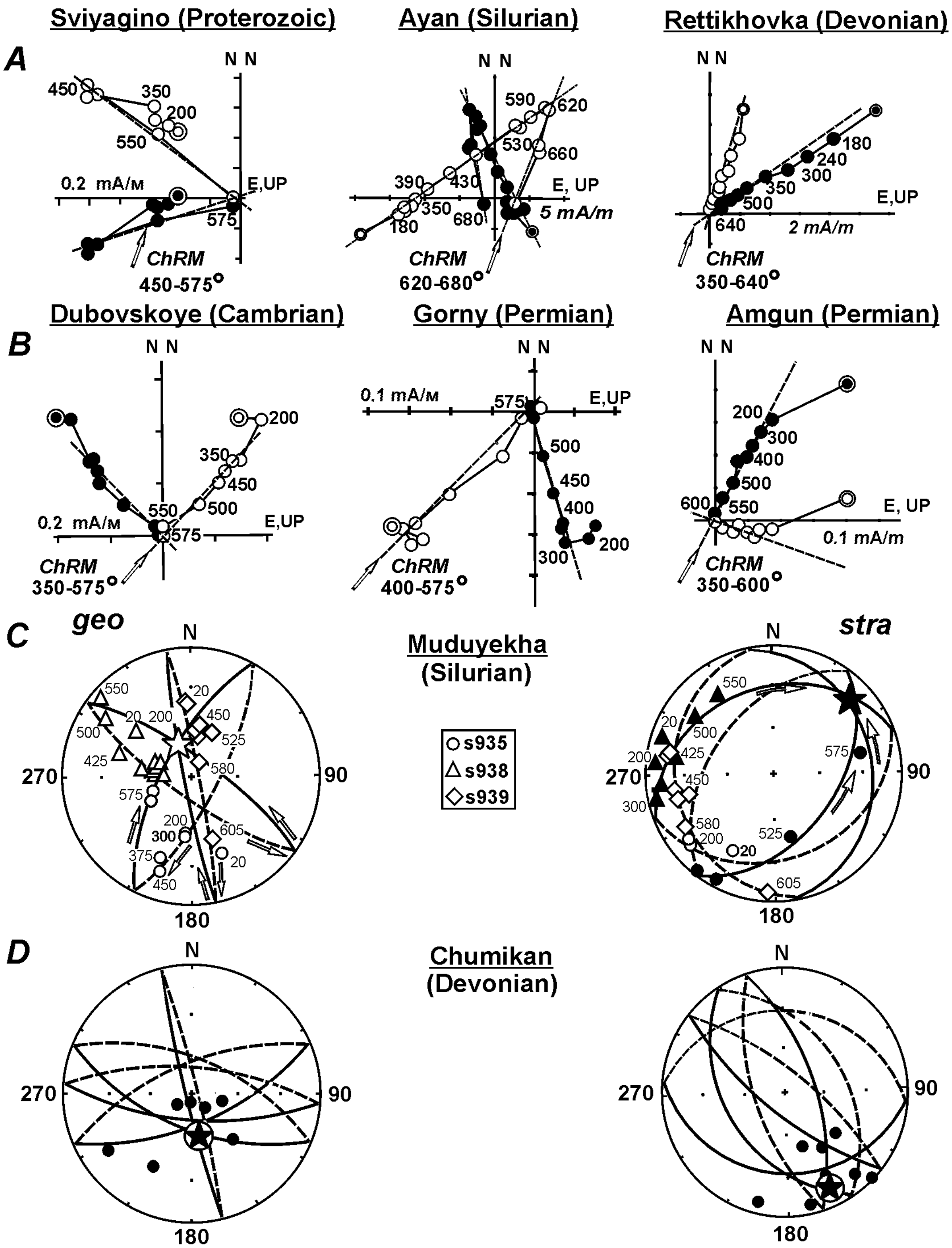

Figure 4. Examples of detecting the characteristic (ChRM) component of the natural remanent magnetization of rocks in the course of temperature cleaning. A and B show the results of the component analysis (CA) [*Kirschvink,* 1980; *Zijderveld,* 1967]; C and D, the results obtained using remagnetization circles (RC) [*Halls,* 1978; *Khramov and Sholpo,* 1967]: (C for individual samples, D for the combination of the CA and RC methods used to determine the average trend. The numbers near the symbols denote the heating temperature, the asterisk marking the average ChRM direction. The solid (empty) symbols denote the projections of the I_n vectors to the horizontal (vertical) plane (N for north, E for east, UP for upward) in the Ziyderveld diagrams, and the projections to the lower (upper) hemisphere, in the stereograms. *geo* and *stra* denote the geographic (modern) and stratigraphic (old) systems of the coordinates, respectively.

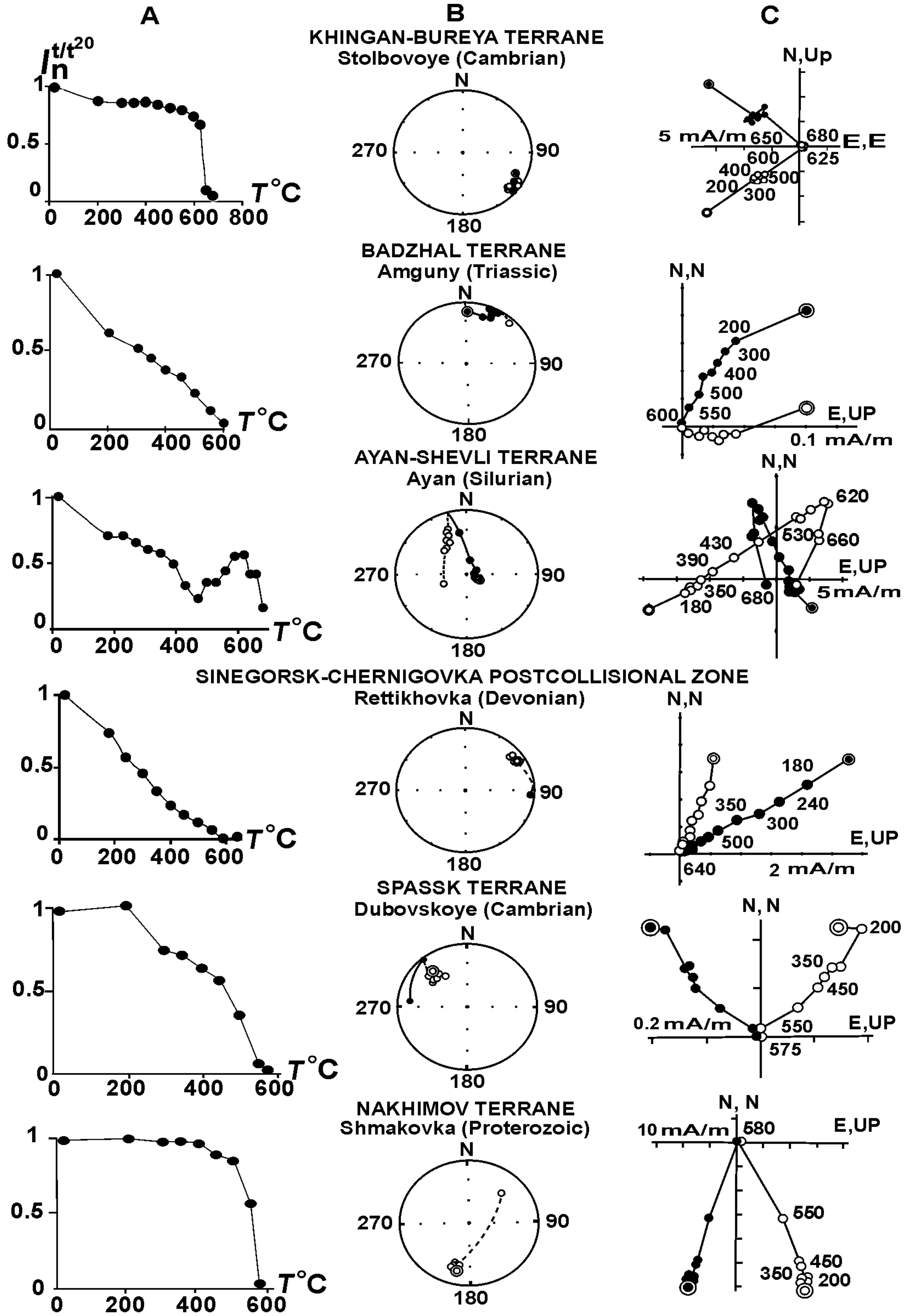

Figure 5. Results of the stepwise thermal demagnetization of the rocks. (A) Typical $I_n(T)$ curves; (B) the stereograms showing the distribution of the magnetization vectors I_n vectors onto the lower and upper hemispheres (solid and empty circles, respectively); (C) the Zijderveld diagrams: the solid (empty) circles denote the projections of the I_n vectors onto the horizontal (vertical) plane, respectively, (N for the north, E for the east, and UP for the upward). The double circles show the initial positions of the I_n vectors. Stratigraphic (old) system of the coordinates.

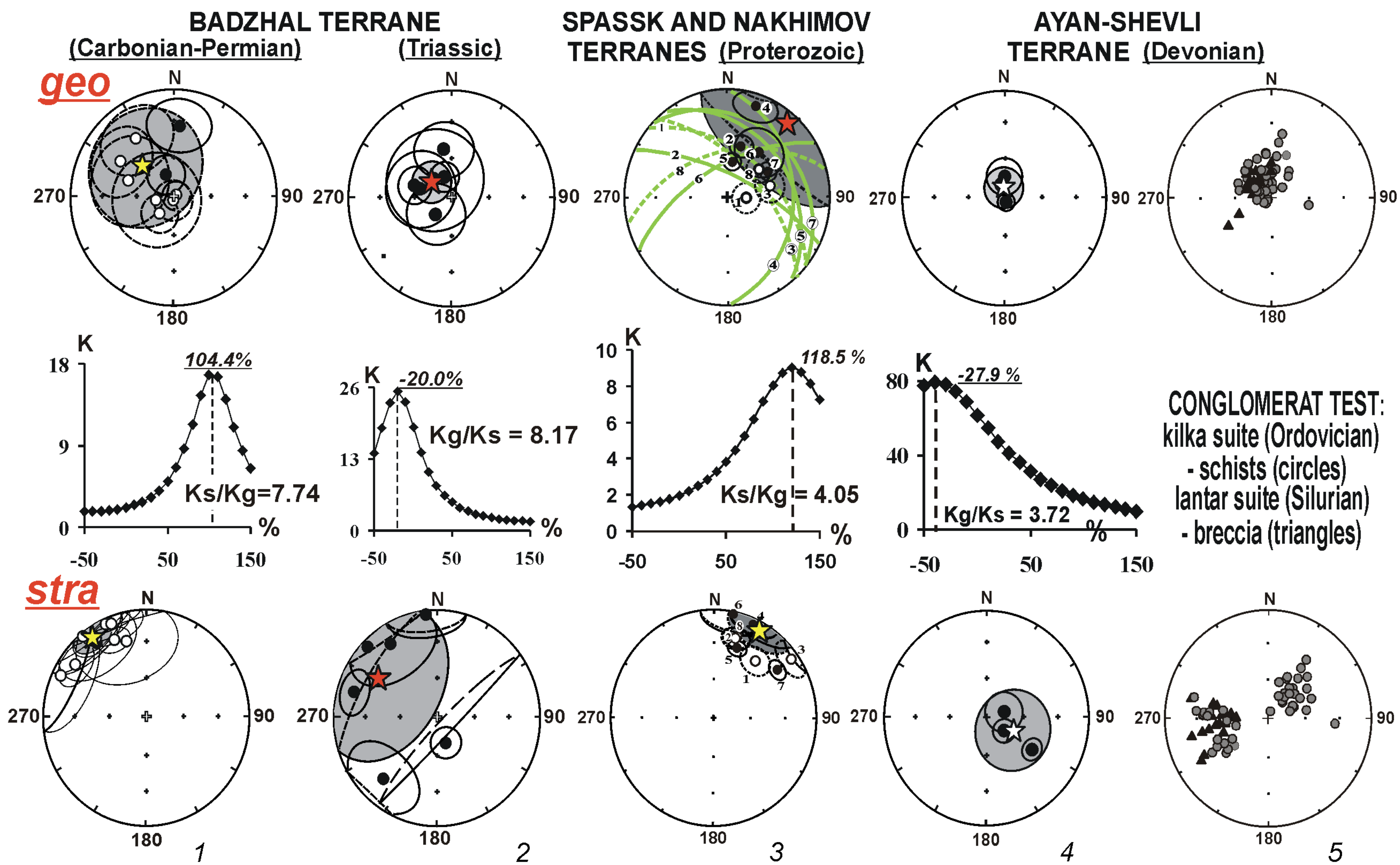

Figure 6. Fold test (1–4) after [*Watson and Enkin,* 1993] and conglomerate test (5) [*Graham,* 1949]: *geo* and *stra* denote the geographic (modern) and stratigraphic (old) systems of the coordinates; the figures (in 3) denote the following Proterozoic-Cambrian rock sequences in the Primorie region: (1) Dubovskoe, (2) Sinii Gai, (3) Kabarga, (4) Krasnyi Kut, (5) Shmakovka, (6) Strelbishche, (7) Sviyagino, and (8) Vysokoe; the solid (broken) lines show the projections of the bedding planes onto the lower (upper) hemisphere. The solid (empty) circles show the projections of the average directions of the identified characteristic magnetization component (ChRM) with confidence ovals onto the lower (upper) hemisphere; the red (yellow) asterisks show the projections of the average trends for the terrains (with shaded confidence ovals) onto the lower (upper) hemisphere; Ks (Kg) denotes the amount of scatter of the vectors in the old (modern) system of the coordinates. The straightening curves in the fold test and the Ks/Kg (Kg/Ks) ratio suggest the relative preservation of the ChRM component.

Table 1. Paleomagnetic characteristics of Paleozoic and Mesozoic rocks in Zabaikalie, Priamurie, and Primorie

no.	Study objects and coordinates	Age	N/n	SYS	D	I	C	A_{95}	φ m	Λ	Φ	dp	dm
	I. ZABAIKALIE												
	Khentei-Dauria Terrain												
1	Tyrin	D	1/12	g	262.6	−15.8	2.6	33.9	−8.1	22.7	−10.9	17.9	34.9
	49.8 112.3			s	254.6	−4.5	3.5	27.0	−2.3	32.7	−11.6	13.6	27.1
2	*Pereval*	D	1/12	g	142.4	−36.1	6.8	18.2	− 20.0	336.1	−47.9	9.2	1.2
	49.8 112.3			s	140.8	11.7	7.1	17.9	5.9	278.4	24.8	68.9	18.2
3	Ulatui	D	1/15	g	236.4	−12.6	3.1	26.3	−6.4	45.1	−26.1	13.6	26.8
	49.8 112.3			s	242.8	−10.6	3.6	23.6	−5.3	40.3	−21.4	12.1	23.9
4	Agutsa	D	2/26	g	244.4	20.0	3.9	16.3	10.3	48.3	8.0	8.9	45.9
	49.4 111.6			s	231.8	5.3	4.4	15.1	2.7	54.4	21.4	13.8	17.1
	Aga Terrain												
5	Onon	D_1	1/6	g	3.3	55.3	15.9	17.6	35.8	235.2	75.0	17.8	25.1
	50.6 155.6			s	31.7	17.0	15.0	18.2	8.7	252.4	40.6	9.7	18.8
6	Ust-Borzya	D_{1-2}	1/11	g	46.7	32.2	4.8	23.4	17.5	230.0	40.3	14.9	26.4
	50.6 115.6			s	48.3	−5.3	5.2	14.4	−2.7	241.7	22.7	11.3	22.6
7	Shazagaitui	D_3-C_1	1/11	g	311.6	26.9	10.0	15.2	14.2	359.3	36.4	9.0	16.5
	51.5 115.1			s	309.8	−31.3	10.3	14.9	−16.9	343.2	8.8	9.3	16.7
8	*Khara-Shibir*	P_1	2/16	g	30.1	2.7	4.7	10.8	1.4	258.2	33.8	9.4	18.8
	51.5 115.3			s	43.4	64.7	9.8	12.5	46.6	197.9	61.6	16.2	20.1
9	Borzya	P_2	6/64	g	209.3	63.4	5.8	30.4	−45.0	276.4	31.5	38.0	48.0
	50.6 116.9			s	205.0	21.3	19.9	15.4	−11.0	269.7	24.6	8.5	16.2
10	Aksha	P_2-T	2/22	g	*144.8	−33.8	6.0	13.8	18.5	347.5	47.5	9.0	15.7
	50.5 113.4			s	*151.2	−16.7	8.6	11.2	8.5	333.1	41.7	6.0	11.6
11	*Khara-Shibir*	T_3	1/7	g	86.0	46.6	16.4	18.5	27.9	189.9	23.8	15.3	23.8
	51.5 115.3			s	273.8	−63.2	14.6	19.6	−44.7	351.5	−31.4	24.3	30.9
	Argun Terrain												
12	Klichka	R_2	2/8	g	92.3	77.5	3.0	29.3	66.1	152.1	43.9	51.4	54.9
	50.4 117.9			s	139.2	8.2	13.9	12.3	4.1	164.0	−25.2	6.2	12.4
13	Georgievka	Є	4/22	g	9.7	−4.6	13.7	8.7	−2.3	287.6	35.6	4.4	8.7
	51.4 119.4			s	10.8	8.7	13.0	8.9	4.4	284.9	42.0	4.5	9.0
14	Makarovo	D	4/39	g	*53.8	5.2	10.9	29.1	2.6	234.3	23.8	14.6	29.2
	51.5 116.0			s	*48.8	20.5	13.4	26.0	10.6	233.9	33.2	14.3	27.3
15	*Khan-Ula*	D	1/25	g	*101.6	−17.8	1.6	36.5	9.1	22.5	14.4	19.6	50.7
	51.2 115.8			s	*118.3	−5.4	4.9	14.6	2.7	4.7	19.5	7.3	14.6
16	Nurinsk-IR	D_3-C_1	2/18	g	45.9	−54.2	4.2	19.3	−34.7	258.9	−4.8	19.0	27.1
	51.1 115.2			s	38.2	−53.7	17.9	8.4	−34.2	264.4	−1.7	8.2	11.7
16a	Nurinsk-AR	D_3-C_1	2/18	g	312.7	−22.9	5.8	15.8	−11.9	343.3	14.8	8.9	16.8
	51.1 115.2			s	318.9	−25.3	8.3	12.8	−13.3	337.0	16.4	7.4	13.8
17	Pavlovsk	D_3-C_1	2/24	g	72.2	9.9	3.7	17.9	5.0	219.3	14.9	9.2	18.8
	51.5 118.3			s	70.1	9.1	3.9	17.3	4.6	221.3	15.9	8.8	17.5
18	*Pavlovsk*	J_1	1/16	g	1.0	63.1	11.1	11.6	44.6	292.4	83.1	14.4	18.3
	51.5 118.3			s	68.4	52.7	10.1	12.2	33.3	200.9	38.4	11.6	16.8
19	Doroga	C	2/11	g	145.0	60.6	9.3	16.2	−41.6	321.3	−7.3	18.8	24.7
	50.8 115.7			s	166.8	21.9	10.7	15.1	−11.4	310.2	26.8	8.4	16.0
20	*Dono*	D	1/9	g	98.5	−59.3	60.9	6.8	−40.1	231.4	−34.8	7.6	10.2
	50.9 115.7			s	19.9	−36.6	55.7	7.1	−20.4	279.2	16.6	4.8	8.3

Table 1. Continued

no.	Study objects and coordinates	Age	N/n	SYS	D	I	C	A_{95}	φ m	Λ	Φ	dp	dm
	II. AMUR REGION												
	Oldoi Terrain												
21	*Urusha*	S	2/21	g	*125.7	22.7	3.0	21.6	−11.8	356.3	9.9	12.2	22.9
	53.9 122.7			s	*128.5	19.4	8.0	11.9	−10.0	354.9	12.8	6.5	12.4
22	*Urusha*	D	2/22	g	*122.0	7.1	3.5	19.6	−3.6	4.0	15.2	9.6	19.0
	53.9 122.7			s	*120.7	−10.2	5.4	14.8	−5.1	10.0	21.8	9.9	19.7
23	*Oldoi*	S	1/8	g	*127.7	−51.3	7.4	21.8	32.0	24.2	47.2	7.6	15.0
	54.0 123.4			s	*130.2	−58.8	10.9	17.6	39.5	30.6	53.9	19.5	26.2
24	*Oldoi*	D	12/135	g	*131.4	−39.7	18.1	10.5	22.5	12.2	42.0	7.6	12.6
	54.0 123.4			s	*137.7	−4.3	23.7	9.1	2.2	358.8	27.7	4.6	9.1
25	*Oldoi*	J	1/5	g	241.9	35.6	5.9	38.2	19.7	67.2	0.7	25.6	44.2
	54.0 123.4			s	233.8	45.3	18.6	20.6	26.8	77.2	3.2	16.6	26.1
26	*Tolbuzino*	J_3	1/8	g	0.5	15.6	19.6	12.8	7.9	304.8	44.8	6.8	13.2
	53.1 125.5			s	3.1	−26.3	20.5	12.5	−13.9	302.2	23.0	7.3	13.5
27	*Albazin*	J_3	1/8	g	351.0	43.8	3.2	36.7	25.6	321.2	61.4	28.6	45.8
	53.4 124.1			s	343.3	4.1	3.4	35.6	2.1	325.1	36.8	17.9	35.7
	Khingan-Bureya Terrain												
28	Soyuznoe	Є	2/25	g	*75.6	−1.8	3.4	18.0	0.9	52.4	−8.9	9.0	18.0
	47.9 131.0			s	*78.8	−0.1	3.8	16.7	0.1	49.4	−7.4	8.4	16.7
29	Stolbovoe	Є	2/16	g	*100.8	16.0	5.6	17.1	8.2	27.5	1.1	9.1	17.6
	48.0 130.9			s	*100.6	−21.3	7.0	15.0	11.0	40.5	15.2	8.3	15.8
30	Teploe Ozero	Є	2/23	g	*162.2	−79.1	3.3	19.1	68.9	114.7	68.2	34.5	36.3
	49.0 131.8			s	*74.4	−18.1	7.5	11.7	9.3	59.8	−3.0	6.3	12.1
31	*Bidzhan*	D	2/25	g	*195.8	−44.5	4.0	16.6	26.2	276.5	65.0	13.1	20.9
	47.9 131.8			s	*183.1	−11.5	4.2	16.2	5.8	307.2	47.8	8.3	16.4
32	*Zeya*	Є	1/7	g	316.9	17.1	3.3	39.3	8.7	3.0	34.2	21.0	40.6
	52.2 128.2			s	283.4	18.8	7.3	24.1	9.7	33.6	15.8	13.1	25.1
33	*Zeya*	S	6/75	g	335.9	87.4	41.5	10.5	84.8	124.3	56.9	20.9	20.9
	52.3 128.2			s	209.8	65.3	4.3	36.5	47.4	108.0	12.8	47.9	59.1
34	*Zeya*	J	3/15	g	2.6	69.2	14.5	10.0	52.8	197.2	88.3	14.5	17.0
	52.4 128.2			s	324.9	70.4	8.7	13.2	54.5	58.6	69.1	19.7	22.8
	Badzhal Terrain												
35	Amgun	D	1/12	g	241.7	−14.1	6.8	17.9	−7.2	64.2	−22.8	9.4	18.3
	51.9 135.6			s	250.4	−0.6	6.8	17.9	0.3	61.4	−11.7	9.0	17.9
36	Amgun	C	5/40	g	326.0	−63.3	2.3	66.0	−44.8	339.4	−11.1	82.2	104.2
	51.9 135.6			s	329.5	−11.1	13.6	21.5	−5.6	350.1	26.9	11.1	21.8
37	Amgun	P	4/31	g	333.9	−53.1	1.5	128.0	−33.7	227.1	1.4	123.0	177.4
	52.1 135.9			s	327.7	−13.9	26.4	18.2	−7.1	351.4	24.9	9.5	18.6
37a	Amgun	C+P	9/71	g	329.7	−59.4	2.2	46.9	−40.2	338.4	−5.8	52.8	70.4
				s	328.7	−12.4	19.4	12.0	−6.3	350.7	26.0	6.2	12.2
37b	*Amgun*	T	6/37	g	305.0	70.0	18.8	15.9	53.9	71.4	57.6	23.5	27.4
				s	301.9	32.1	2.3	57.3	17.4	30.9	33.1	36.3	64.5
	Kiselevka-Manoma Terrain												
38	*Kiselevka*	J_3-K_1	3/28	g	295.0	4.4	31.1	5.0	2.2	30.4	17.1	2.5	5.0
	51.4 139.1			s	296.4	−32.8	26.4	5.4	−17.9	17.6	1.4	3.5	6.1
	Khabarovsk Terrain												
39	*Most*	P	1/10	g	324.3	63.6	79.2	6.6	45.2	50.8	65.5	8.3	10.5
	48.5 135.0			s	323.8	6.9	13.2	16.1	3.5	1.3	35.4	8.1	16.2

Table 1. Continued

no.	Study objects and coordinates	Age	N/n	SYS	D	I	C	A_{95}	φ m	Λ	Φ	dp	dm
	Galama Terrain												
40	*Chumikan*	Є	2/15	g	119.5	70.1	4.0	21.4	54.1	171.6	29.5	31.8	36.9
	54.6 135.7			s	118.2	28.2	5.2	18.4	15.0	194.2	−3.1	11.1	20.2
41	*Chumikan*	S	3/27	g	167.0	41.0	5.4	13.0	23.5	147.8	−11.1	9.6	15.8
	54.6 135.7			s	153.0	11.3	4.6	14.4	5.7	165.8	−25.6	7.4	14.6
42	*Chumikan*	D	2/17	g	54.6	−25.6	13.0	9.6	−13.5	262.6	7.8	5.6	10.4
	54.6 135.7			s	28.2	−33.0	11.9	10.1	−18.0	288.2	13.5	6.5	11.5
	Ayan-Shevli Terrain												
43	Ayan	O?kl	5/82	g	254.0	26.2	2.0	73.4	13.8	69.0	2.8	43.0	79.4
	56.2 138.2			s	260.8	17.3	6.6	32.2	8.9	60.7	2.3	17.2	33.3
43a	Ayan		1/10	g	224.3	−28.4	5.0	24.2	−15.1	80.7	−37.0	14.6	26.6
				s	225.1	9.2	8.2	17.9	4.6	89.9	−18.9	9.1	18.1
44	Ayan	S_{1-2}ln	1/18	g	301.9	71.5	35.4	5.9	56.2	73.0	58.7	9.1	10.3
				s	264.9	46.2	26.6	6.8	27.5	68.3	19.9	5.6	8.7
45	Ayan	D_1?uk	5/75	g	272.1	82.8	13.0	22.0	75.8	113.5	54.2	42.0	43.0
				s	212.5	68.2	2.7	58.4	51.3	117.2	20.8	82.6	98.2
45a	Ayan	J_3-K_1	3/36	g	353.2	82.6	61.7	15.8	75.4	133.1	70.6	30.1	30.8
				s	116.3	65.5	16.6	31.2	47.7	180.7	26.6	41.2	50.7
	III. PRIMORIE Nakhimovsk Terrain												
46	Orlovka	PЄ	1/17	g	*101.6	−68.3	39.5	7.1	51.5	80.7	40.2	10.1	12.0
	45.4 133.7			s	*55.3	−49.0	39.5	7.1	29.9	88.2	0.5	6.2	9.4
47	Shmakovka	PЄ	1/12	g	188.7	−62.5	12.0	13.1	−43.8	53.6	−83.6	16.0	20.5
	45.3 133.5			s	199.4	−31.3	42.7	6.8	−16.9	97.5	−57.3	4.3	7.6
48	Sviyagino	PЄ	1/21	g	239.4	−51.3	20.9	7.1	−32.0	37.7	−42.8	6.5	9.6
	44.9 133.2			s	234.3	−23.5	21.6	7.0	−12.3	60.8	−33.6	4.0	7.5
49	Kabarga	PЄ -Є	1/18	g	256.2	54.2	8.2	12.8	34.7	77.7	15.5	12.6	18.0
	45.4 133.6			s	233.9	6.2	8.9	12.3	3.1	73.1	−22.0	6.2	12.4
50	Strelbishche	PЄ -Є	1/22	g	*37.4	46.0	3.6	19.3	−27.4	62.1	−55.4	15.8	24.7
	45.4 133.7			s	*11.6	1.3	3.6	19.3	−0.7	117.4	−44.1	9.7	19.3
	Spassk Terrain												
51	*Khalkidon*	Є	2/31	g	*121.2	−69.9	34.0	4.5	53.8	78.4	51.5	6.6	7.7
	44.3 132.4			s	*152.7	−9.6	5.9	11.7	4.8	351.7	43.8	6.0	11.8
52	Vysokoe	Є	1/7	g	*50.7	−56.8	13.9	16.8	37.4	94.5	3.7	17.7	24.4
	44.3 132.5			s	*16.2	−23.3	38.0	9.9	12.2	113.7	−31.7	5.6	10.5
53	Dubovskoe	v	2/22	g	*93.3	−74.8	6.7	13.0	61.5	94.7	39.5	21.6	23.7
	44.6 132.9			s	*37.4	−32.8	8.2	11.5	17.9	95.2	18.8	7.4	13.0
54	Spassk	Є	1/11	g	*104.5	−31.0	–	12.0	16.7	45.2	21.9	7.5	13.4
	44.6 132.8			s	*17.7	−49.2	–	12.8	30.1	117.2	−13.6	11.2	17.0
55	Klyuchi	Є	1/24	g	299.5	−62.6	8.7	12.8	−44.0	352.9	−13.5	15.7	20.0
	44.4 132.8			s	266.4	−0.2	11.7	11.0	−0.1	45.3	−2.6	5.5	11.0
56	Gai	Є	1/16	g	*16.7	48.7	14.0	10.3	29.6	85.1	−70.2	8.9	13.6
	44.5 132.6			s	*16.5	−22.5	17.5	9.1	11.7	113.5	−31.9	5.1	9.6
57	Khutor	Є	1/16	g	271.4	55.3	43.1	7.6	35.8	69.3	25.0	7.7	10.8
	44.3 132.7			s	277.2	10.3	46.5	7.3	5.2	41.4	8.8	3.7	7.4

Table 1. Continued

no.	Study objects and coordinates	Age	N/n	SYS	D	I	C	A_{95}	φ m	Λ	Φ	dp	dm
	Laoelin-Grodekovo Terrain												
58	Starateli	S_1	1/17	g	*51.0	58.7	13.2	10.2	−39.4	30.1	−52.3	11.3	15.2
	44.1 131.2			s	*69.0	20.7	9.9	11.9	−10.7	48.1	−22.5	6.6	12.5
59	Muduyekha	S_1	1/19	g	*43.8	66.4	8.4	12.3	−48.9	16.8	−59.9	16.6	20.2
	44.2 131.4			s	*65.8	0.7	9.0	11.8	−0.4	58.5	−17.3	5.9	11.8
60	Kordonka	S_1	1/13	g	*52.7	−72.7	10.1	12.3	58.1	104.5	21.3	19.4	21.9
	44.3 131.3			s	*85.3	−24.0	10.8	11.8	12.6	53.6	5.4	6.7	12.6
61	*Zastava*	S	1/19	g	359.1	29.0	6.5	13.9	15.5	313.1	61.2	8.4	15.3
	44.3 131.3			s	353.5	3.5	4.4	17.5	1.8	320.9	47.1	8.8	17.5
	Sinegorsk-Chernigovka zone of post-collision rocks												
62	Buyanki	O-S	2/34	g	194.9	25.5	7.2	12.3	13.4	116.0	−30.8	6.9	12.8
	44.2 132.9			s	208.2	5.8	7.7	11.9	2.9	96.9	−36.6	6.0	11.9
63	Kremovo	O-S	1/25	g	231.9	−77.7	37.8	6.3	−66.4	345.1	−54.5	11.1	11.8
	44.0 132.3			s	222.3	−18.3	29.9	7.1	−9.4	72.7	−39.7	3.8	7.4
64	Vinogradovka	D_{2-3}	3/21	g	303.9	−16.3	9.2	11.1	−8.3	12.3	17.3	5.9	11.4
	43.8 132.9			s	302.8	20.1	7.9	12.0	10.4	26.8	30.6	6.6	12.6
65	Anikin Klyuch	D_{2-3}	2/18	g	246.9	−32.1	7.8	13.2	−17.4	45.3	−28.5	8.4	14.9
	43.7 132.5			s	250.3	−43.5	8.1	13.0	−25.4	35.8	−31.1	10.1	16.2
66	Retikhovka	D_{2-3}	1/26	g	*82.8	38.1	27.1	7.2	−21.4	31.7	−19.8	5.0	8.5
	44.2 132.7			s	*70.1	−11.5	31.4	6.7	5.8	61.0	−9.9	3.5	6.8
67	*Artem*	D_{2-3}	2/18	g	329.5	9.3	11.1	10.9	4.7	356.0	42.8	5.6	11.0
	43.4 132.4			s	319.2	12.4	15.4	9.1	6.3	8.4	38.4	4.7	9.3
68	*Artem*	P_2	2/19	g	272.7	75.4	4.9	16.8	62.5	96.1	38.6	28.2	30.8
	43.3 132.3			s	211.8	51.1	16.7	8.5	31.8	105.3	−9.5	7.8	11.5
69	*Mramor*	C-P	2/41	g	12.1	58.1	18.2	5.4	38.8	239.4	80.1	5.9	8.1
	42.6 130.8			s	48.8	31.1	17.6	5.5	16.9	237.2	41.4	3.4	6.2
70	*Gornyi*	P_2	1/22	g	*64.5	79.4	24.0	6.5	−69.5	343.6	−50.0	11.8	12.4
	44.7 134.0			s	*161.9	38.7	25.8	6.2	−21.8	332.0	21.4	4.4	7.4
71	*Gornyi*	T	1/14	g	357.1	78.5	51.2	5.6	67.9	131.2	66.9	10.0	10.6
	44.8 134.0			s	262.6	52.7	47.9	5.8	33.3	73.3	18.1	5.5	8.0
72	*Breevka*	T_3-J_1	2/13	g	282.8	69.6	43.0	39.1	53.4	83.6	40.9	57.3	66.9
	43.2 133.9			s	296.4	16.1	91.7	26.4	8.2	30.9	24.5	14.0	27.2
73	*Russkii*	T_{1-2}	2/13	g	325.6	55.5	10.6	13.4	36.0	38.8	62.8	13.7	19.1
	43.0 131.9			s	324.8	58.0	10.9	13.1	38.7	44.7	63.2	14.2	19.3
74	*Tri Kamnya*	T_1	1/10	g	333.9	60.8	4.1	27.2	41.8	47.0	70.8	31.7	41.6
	43.2 132.1			s	37.4	73.8	3.9	28.2	59.8	172.6	62.0	45.7	50.8
75	*Smidovich*	T_2	1/9	g	316.2	34.9	4.6	26.9	19.2	23.0	46.2	17.8	31.0
	43.3 132.2			s	297.1	53.9	5.4	24.5	34.4	54.0	41.4	24.0	34.3
76	*Mnogoudobnoe*	T_3	1/13	g	329.9	20.2	4.3	22.8	10.4	359.8	47.9	12.5	23.9
	43.5 132.5			s	331.7	71.5	4.4	22.4	56.2	87.7	68.0	34.4	39.3
	Khor Block												
77	*Khor*	P	3/36	g	233.0	−39.0	17.6	6.0	−22.0	58.0	−40.8	4.3	7.2
	47.7 136.3												

Table 1. Continued

no.	Study objects and coordinates	Age	N/n	SYS	D	I	C	A_{95}	φ m	Λ	Φ	dp	dm
	Sergeevka Terrain												
78	<u>Anna</u>	Є	2/17	g	159.2	64.3	6.0	19.3	46.1	146.8	0.8	24.7	30.9
	42.9 132.6			s	144.4	3.8	6.3	18.8	1.9	177.8	−35.0	9.4	18.8
79	<u>Yastrebovka</u>	Є	2/28	g	152.9	−10.1	3.7	21.8	−5.1	173.4	−45.0	11.2	22.1
	43.2 133.5			s	150.1	26.6	9.4	12.8	14.1	166.2	−26.5	7.5	13.9
80	Orel	Є	1/24	g	292.7	27.0	7.5	13.6	14.3	38.4	26.2	8.1	14.8
	43.2 133.3			s	318.1	28.8	16.9	9.3	15.3	18.5	44.8	5.6	10.3
81	*Vodopadnyi*	Є	1/11	g	80.3	−19.5	16.3	13.6	−10.0	236.2	0.1	7.4	14.2
	43.1 132.3			s	285.7	15.3	16.3	13.6	7.8	37.3	16.8	7.2	14.0
82	*Ekaterinovka*	Є	1/11	g	322.0	21.2	25.6	10.1	11.0	10.5	44.1	5.6	10.6
	43.0 133.1			s	206.5	−5.2	8.2	18.0	−2.6	95.8	−4.3	9.1	18.1

Note. Age abbreviations: PЄ – Precambrian, Є – Cambrian, O – Ordovician, S – Silurian, D – Devonian, C – Carboniferous, P – Permian, T – Triassic, J – Jurassic; N/n – number of geologic sections/lump samples used to identify I_n components by cube-based averaging; SYS (g, s) denotes the geographical (modern) and stratigraphic (old) systems of the coordinates; D and I denote the declination and inclination of the average vector of the high-temperature ChRM component identified during the determination of the paleomagnetic pole; C is the cluster distribution of unit ChRM vectors; A_{95} is the confidence circle radius for the average vector with p=0.95; Cs/Cg is the ratio of the clusters in the old (Cs) and modern (Cg) systems of the coordinates; φm, Φ, Λ, and (dp, dm) denote the geomagnetic latitude (paleolatitude) of the region, and the longitude and latitude (the semiaxes of the confidence circle) of the paleomagnetic pole. The asterisks denote the values which were reversed by 180 degrees later when determining the northern paleomagnetic pole. Underlined are the adjacent rock sequences which gave a positive fold test and were used to calculate the average poles. Given in italics are the objects for which the calculated pole positions are preliminary or problematic (the identified ChRM component reflects the situations where the rocks show merely post-folding magnetization, or the sum of the pre- and post-folding magnetization components, both for some individual rock sequences, and in the case of their grouping. The Nura-AR(IR) unit is represented by the Argalei Formation (Iram rock sequence).

et al., 1985; *Lin et al.,* 1985; *Ma et al.,* 1993; *Meng and Coe,* 1992; *Wu et al.,* 1993; *Yang et al.,* 2002; *Zhao et al.,* 1992, 1993, 1996; *Zhenyu et al.,* 1999; *Zhu and He,* 1987]. However, these data are often different and contradictory in terms of the paleopole position [e.g., *Huang et al.,* 2000; *Zhao et al.,* 1993]., this being not always caused by the preferred choice of some or other polarity (this being problematic for the Early-Middle Paleozoic). The coincidence of these paleopoles, recorded for the Silurian-Devonian rocks, with the faunally and statistically proved positions of the North China Platform in the Permian-Carboniferous and Mesozoic periods of time [*Enkin et al.,* 1992; *Gilder and Courtillot,* 1997; *Pruner,* 1987; *Yang et al.,* 1991, 1992] provides, in our opinion, a good basis for believing that these rocks were remagnetized during the time of the Hercynian-Cimmerian orogenesis. This applies to many of the rock sequences we investigated in the Mongolia-Okhotsk and Sikhote-Alin foldbelts, where the large-scale Late Paleozoic-Mesozoic remagnetization had taken place, and also to the rocks reported in [*Kravchinsky et al.,* 2002]. The latter authors described the positions of the Devonian paleopole determined using the rocks of several rock sequences determined using the rocks of several geologic sections, exposed by the Oldoi River in the Amur R. area, the magnetization of which is believed by these authors to be a primary one. The differences between the resulting positions of the Silurian-Devonian paleopole and the results of other researchers, for instance [*Zhao et al.,* 1993], are explained by *Kravchinsky et al.* [2002] by the potential rotations of the blocks around a vertical axis in the sampling site, see a light-color, striated arc-shaped band (see plate 4 in Figure 7.) No geological explanation was found for this rotation by 90°–120° even in terms of the fault tectonics analysis. This interpretations seems to be insufficiently substantiated also in the paleomagnetic aspect: the results of the fold test were not quite correct because they were based on the recording negative polarity and on the use of some formal numerical parameters which were not quite strict in terms of the McElhinny [*McElhinny,* 1964] and Watson and Enkin [*Watson and Enkin,* 1993] tests. Neither were they subjected to the "powerful", mathematically and geophysically substantiated tests offered by [*McFadden,* 1990; *Shipunov,* 1995a; *Shipunov and Bretshtein,* 1999; *Shipunov and Muraviev,* 2000]. Hence, the detailed age gradation of the Devonian poles is unjustified. Our paleomagnetic study of the same Devonian rocks using the geological rock sequences of the Oldoi R. and Urusha R. basins, which exceed the sample collections of the geologists mentioned above both in space and number, confirmed the paleomagnetic trends obtained previously (Figures 7, where the Silurian and Devonian rocks are shown in different colors), yet they are insufficient to grade the data, as offered without proof in [*Kravchinsky et al.,* 2002]. Yet, the more important fact is that these poles coincide wholly with the areas which include the paleopoles obtained for the Late Paleozoic and Mesozoic rocks. The same applies to the Silurian and Devonian paleopole positions reported in [*He et al.,* 1988; *Huang et al.,* 2000; *Li et al.,* 1985; *Meng and Coe,* 1992; *Yang et al.,* 2002; *Zhenyu et al.,* 1999; *Zhu and He,* 1987], which "coincide" well with the younger Mesozoic poles and differ from the poles obtained in our study and reported in [*He et al.,*

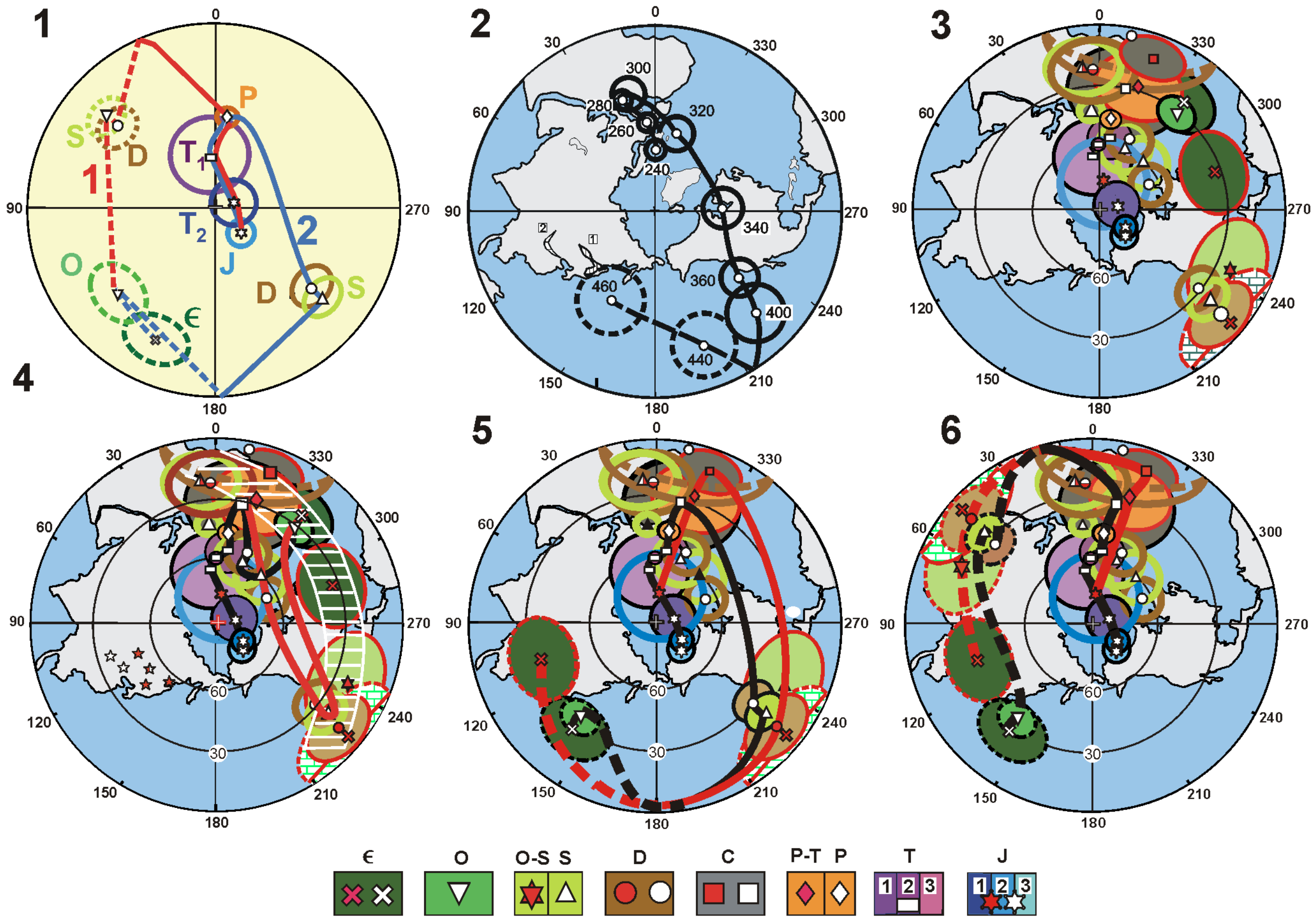

Figure 7. The positions of the paleomagnetic pole and the analysis of the potential paths of its apparent movement (APMP) in the Phanerozoic. APMP for the North China Plate (NCP): (1) two versions (1) after [*Zhao et al.,* 1992] and (2) after [*Pecherskii and Didenko,* 1995], the numbers denoting the age in Ma; (3–6) the positions of the paleopole and those of the APMP for NCP after [*He et al.,* 1988; *Huang et al.,* 1999, 2000; *Kravchinsky et al.,* 2002; *Meng and Coe,* 1992; *Zhao et al.,* 1992; *Zhu and He,* 1987] (white symbols and black lines, respectively), as well as the positions of the terranes in the orogenic belts of the Far East (Russia) and Zabaikalie (red symbols and lines): (3) APMP after [*Huang et al.,* 1999]; (4) same after [*Huang et al.,* 2000]. The white "staircase" shading denotes the direction inferred by [*Kravchinsky et al.,* 2002] of the adjacent geoblocks along the arc of a small circle around the Euler pole (shown by a rhomb) by 90–120°; (5–6) the APMP versions used in choosing different polarities of the geomagnetic field in the Early-Middle Paleozoic. The shapes of the symbols and the color (or shading) of the confidence ovals agree with the legend for the geological ages. The positions of the paleopoles for the Cambrian rocks of the Khingan-Bureya Terrane ("brick" hatching of the confidence ovals), as well as for the Silurian and Devonian rocks (thicker open confidence ovals), agree with groups of some individual rock sequences the paleomagnetic age of which may reflect syn- and post-folding remagnetization, or the local rotation of the geoblocks. The solid (broken) APMP lines show the projections onto the upper (or lower) hemisphere. The stars show the main areas of sample collecting. The ages of the rocks are: (E) Cambrian, (O) Ordovician, (S) Silurian, (D) Devonian, (C) Carboniferous, (P) Permian, (T) Triassic, and (J) Jurassic.

1988; *Zhao et al.,* 1993]. Moreover, the location of the paleopole reported in [*Zhao et al.,* 1993] and the data obtained by *Huang et al.* [2000] belong to the rocks of the same age found in the areas spaced a few dozens of kilometers apart.

It follows that the similarity of the positions of some paleopoles of the Middle Paleozoic objects with those of the Mesozoic ones suggests a simpler obvious explanation of this fact by Mesozoic remagnetization during the accretion-collision folding. On the other hand, the polarity version assumed by us for the case of the Cambrian rocks in the Khingan-Bureya terrane gives the anomalous position of the Cambrian paleopole compared to the other terranes of the

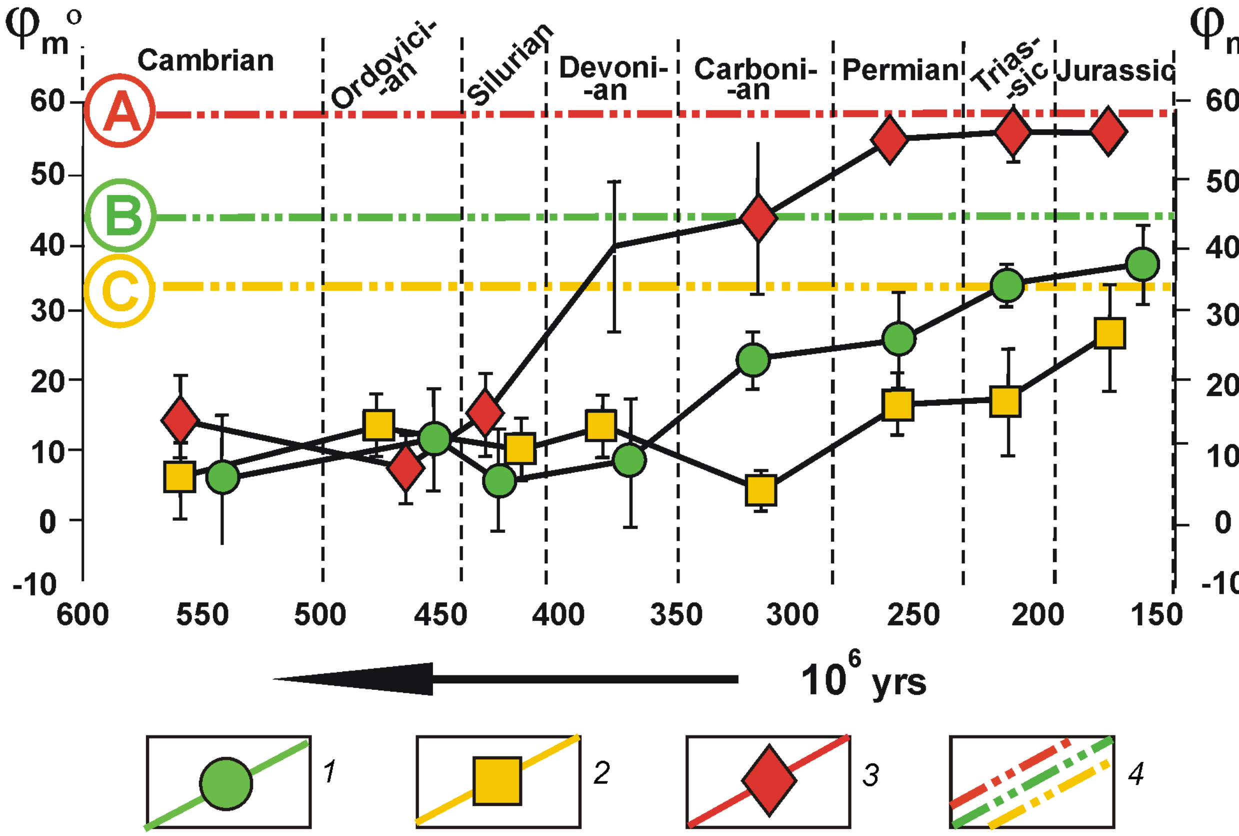

Figure 8. Comparison of the paleolatitudes where the terranes were formed in the Southern Far East of Russia (1) and in the North China (2) and Siberian (3) plates. (4) The average modern geographical latitude of Siberia (A), the regions of study in Primorie and Priamurie (B), and North China (C).

Sea of Okhotsk coast and the East Baikal region which coincides with the position of the pole for Devonian time. It remains to infer potential remagnetization during the Devonian or the erroneous dating of geological time, which is quite probable for the region concerned because of its poor knowledge.

Worthy of note is the poor situation with getting high-quality, unambiguous pole locations for the Late Triassic and Jurassic rocks, showing a significant scatter for some rock sequences. In any case, the positions of the Jurassic paleopole for some objects, for instance, for the tuffaceous-sedimentary and volcanic rocks of the Uda volcanic belt, are closer to the Siberian poles compared to those of North China. This might have been caused by the fact that the volcanic rocks of the Uda Arc belonged by that time to the stable continental margin (pericratonic trough) of the Siberian plate.

It should be emphasized that the displacement trends of the paleopole positions for the terranes of the Mongolia-Okhotsk and Sikhote-Alin foldbelts, as well as for the North China Platform, being similar in many respects to one another, differ essentially, beginning from the Middle Paleozoic, from the apparent motion path of the paleopole for the Siberian Plate [*Khramov et al.,* 1982], reflecting differences in the positions of the terranes belonging to the Mongolia-Okhotsk and Sikhote-Alin foldbelts, as well as that of the North China Plate, relative to the position of the Siberian Platform. The restriction of these terranes during the Early-Middle Paleozoic to a twenty-degree zone of subtropic paleolatitudes bordering the equator (Figure 8) agrees with the recent reviews and geodynamic generalizations, as well as with the biostratigraphic data available for the Sikhote-Alin and Mongolia-Okhotsk regions. Although the Angarian flora found in the Permian rocks of the Trans-Baikal region suggests the higher, moderate paleolatitudes, compared to the paleomagnetic data [*Parfenov et al.,* 1999]. Discrepancies of this kind can be explained by the overlapping of various fauna and flora references in time and space in migrating ecotones [*Dubatolov,* 2002], or by the inaccurate (not exact) age determinations available for the rocks of the compared objects (for example, in the Maritime Territory). Yet, remagnetization cannot be excluded.

A great difference between the Middle and Late Paleozoic latitudes of the Siberian and North China plates [*Khramov et al.,* 1982; *Pecherskii and Didenko,* 1995] controlled the "intermediate" positions of many Mongolia-Okhotsk and Sikhote-Alin terrains in the Paleozoic Paleoasian Ocean. The scatter of the paleolatitude values for the end of the Paleozoic to the beginning of the Mesozoic is a remarkable fact which calls for additional studies. Figure 8 shows merely the paleolatitudes averaged for the whole region (for all terranes where the rocks of the respective ages were investigated), which have been assigned conventionally to the mid-

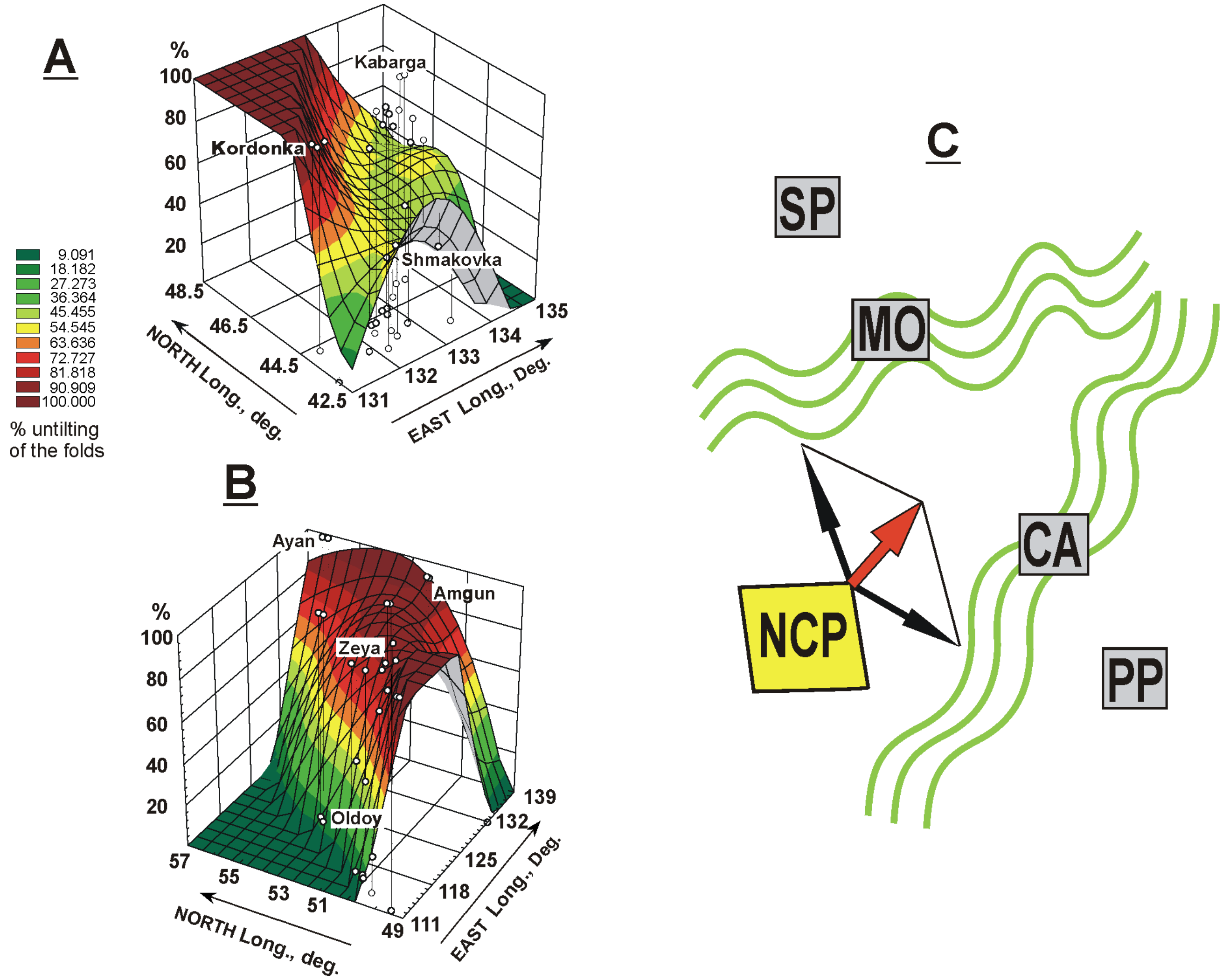

Figure 9. Preliminary estimates for the completion degree of the deformation (in %) of the Mongolia-Okhotsk (A) and Sikhote-Alin (B) superterrains by the time of the development of secondary (post-folding) magnetization (after [*Shipunov,* 1995b]. 3-D diagrams: A(B) Sikhote-Alin (Mongolia-Okhotsk) superterranes; dots denote individual geologic sections; C potential trends of stress and remagnetization development in the fold zones of the Mongolia-Okhotsk (MO) and Sikhote-Alin (SA) foldbelts; SP, NCP, and PP denote the Siberian, North China, and Pacific plates, respectively.

dles of the respective geologic periods. Any more detailed analysis of the latitudes at the present-day knowledge would be speculative and not sufficiently substantiated.

All of these data testify to the fact that we still have a problem both in terms of getting high-quality paleomagnetic inwestigations and their objective interpretation for the whole region of the Asian-Pacific continental margin.

It can be noted, in conclusion, that proceeding from the interrelationship (in time and space) between the orogenic processes and geomagnetic field variations, the trend of folding intensity in time and space may correlate with the different degrees of the preservation of pre-, syn-, and post-folding ChRM components. Some of the paleomagnetic criteria developed for the quantitative estimation of this relationship [*Shipunov,* 1995b] allow one to estimate the scales and trends of these processes. Our preliminary estimation of the degree of folding completion depending on the character and size of the manifestation (preservation) of the pre-, syn-, and post-folding magnetization components showed that in the case of the Phanerozoic rocks of the Mongolia-Okhotsk superterrane the general development of the deformation evolution front proceeded mainly from SSE to NNW, whereas in the case of the rock sequences of the Sikhote-Alin superterrane the general trend of folding development was almost opposite more complicated (Figure 9). Since the spatial manifestation of synfolding magnetization turned out to be almost of the same type, it can be concluded that the main phase of folding and remagnetization seems to have been operating at the beginning of the Mesozoic, or at least not earlier than the late Permian. These date are in good agreement with the general geological views on the character and trend of accretion-collision processes that operated at the contact between the Siberian and North China plates, if we assume the drifting (overthrusting) of the latter in the general NE direction and its "wedging" into the terrigenous rock sequences of the Mongolia-Okhotsk and Sikhote-Alin foldbelts which show a face-to-face connection and surround the Siberian and Pacific more rigid plates. This might have caused the almost opposite spacial trend of remagnetization (against the general background of the progressing stress and crumpling of the sedimentary rocks). The probability of this scenario is confirmed by the general character of the development of orogenic structures in the Mongolia-Okhotsk and Sikhote-Alin fold belts throughout the Late Paleozoic and Mesozoic period of time [*Nagibina,* 1963; *Natal'in,* 1991; *Parfenov et al.,* 1996].

Acknowledgments. We are grateful to Professor D. M. Pecherskii for his reading this paper and suggesting some useful comments.

References

Bazhenov, M. L., G. Z. Gurarii, O. A. Krezhovskikh, and A. G. Fein (1999), Paleomagnetic studies of Permian and Mesozoic rocks in Southern Primorie, in *Theoretical and Regional Problems of Geodynamics,* pp. 181–195, Nauka, Moscow.

Bretshtein, Yu. S. (1988), Magnetic properties of Late Cretaceous-Cenozoic volcanic rocks in the Soviet Far East South, *J. Phys. Earth Int., 36,* 39–64.

Bretshtein, Yu. S. (1991), Magnetic characteristics of basaltic rocks as indicators of volcanic environments with reference to the northwestern Circum-Pacific mobile belt, *Geol. Pacific Ocean, 6*(6), 1369–1392.

Bretshtein, Yu. S., G. Z. Gurarii, and D. M. Pecherskii (1999), Paleomagnetism of Paleozoic rocks in the terrains of Southwest Primorie, *Geol. Pacific Ocean, 4*(4), 545–585.

Bretshtein, Yu. S., Yu. D. Zakharov, and A. V. Klimova (2003), Paleomagnetic study of Triassic rocks in Southern Primorie, *Pacific Geology,* (1), 71–82.

Dobson, J. P., and F. Heller (1992), Remagnetization in Southeast China and the collision and suturing of the Huanan and Yangtze blocks, *Earth Planet. Sci. Lett., 111,* 11–21.

Dubatolov, V. N., and V. I. Krasnov (2002), *The Devonian Paleoclimates in the Asian Part of Russia,* pp. 3–77, SNIIGIMS, Novosibirsk.

Enkin, R. J., Z. Yang, Y. Chen, and V. Courtillot (1992), Paleomagnetic constraints on the geodynamic history of the major blocks of China from the Permian to the Present, *J. Geophys. Res., 97*(1), 13,953–13,989.

Gao, R. F., H. L. Huang, Z. W. Zhu, et al. (1983), The study of paleomagnetism in the Northeastern Sino-Korean Massif during the pre-Late Paleozoic, in *Contr. Project of Plate Tectonics in North China,* vol. 1, pp. 265–274, Geol. Publ. House, Beijing.

Gilder, S., and V. Courtillot (1997), Timing of the North-South China collision from new Middle to Late Mesozoic paleomagnetic data from the North China block, *J. Geophys. Res., 102*(B8), 17,713–17,727.

Graham, J. W. (1949), The stability and significance of magnetism in sedimentary rocks, *J. Geohys. Res., 54,* 131–167.

Halls, H. C. (1978), The use of converging remagnetization circles in paleomagnetism, *Phys. Earth Planet. Inter., 16,* 1–11.

He, Z. X., Z. C. Zheng, and H. Zhu (1988), A preliminary research into the paleomagnetism of the Paleozoic strata in the Hexizouland Massif, *Geoscience, 2,* 186–193.

Hodych, J. P., S. Bijaksana, and R. Patzold (1999), Using magnetic anisotropy to correct for paleomagnetic inclination shallowing in some magnetite-bearing deer-sea turbidites and limestones, *Tectonophysics,* (307), 191–205.

Huang, B., Z. Y. Yang, Otofuji Yo-ichiro, and R. X. Zhu (1999), Early Paleozoic paleomagnetic poles from the western part of the North China block and their implications, *Tectonophysics, 308,* 377–402.

Huang, B., Otofuji Yo-ichiro, Z. Yang, and R. Zhu (2000), New Silurian and Devonian paleomagnetic results from the Hexi Corridor terrain, Northwest China, and their tectonic implications, *Geophys. J. Int.,* (140), 132–146.

Huang, B., Otofuji Yo-ichiro, R. Zhu, R. Shi, et al. (2001), Paleomagnetism of Carboniferous sediments in the Hexi Corridor: Its origin and tectonic implications, *Earth Planet. Sci. Lett.,* (194), 135–149.

Johns, M. P., A. I. Kirker, and F. McClelland (1997), Deflection of magnetic remanence during progressive cleavage development in the Pembrokeshire old red sandstones, *Geophys. J. Int., 130,* 240–250.

Kent, D. V., Z. Xiangshan, Z. W. You, and N. D. Opdake (1987), Widespread Late Mesozoic to Recent remagnetization of Paleozoic and Lower Triassic sedimentary rocks from South China, *Tectonophysics, 139,* 133–143.

Khramov, A. N., G. I. Goncharov, R. A. Komissarova, et al. (1982), *Paleomagnetology,* 312 pp., Nedra, Leningrad.

Kim Bang Yeon and P. Kodama Kenneth (2004), A compaction correction for the paleomagnetism of the Nanaimo Group sedimentary rocks: Implications for the Baja British Columbia hypothesis, *J. Geophys. Res., 109*(B02102), doi:10.1029/2003JB002696.

Klimova, A. V., and Yu. S. Bretshtein (1993), Magnetism of Cenozoic basaltoids from the Middle Amur area, *Geol. Pacific Ocean, 9*(1), 64–77.

Kirschvink, J. I. (1980), The least-squares line and plane and the analysis of paleomagnetic data, *Geophys, J. R. Astron. Soc., 62,* 699–718.

Kravchinsky, V. A., A. A. Sorokin, and V. Courtillot (2002), Paleomagnetism of Paleozoic and Mesozoic sediments from the southern margin of the Mongolia-Okhotsk ocean, Far East Russia, *J. Geophys. Res., 107*(B10), 22–53.

Kurilenko, A. V., Yu. S. Bretshtein, and K. S. Butin (2001), New biostratigraphic and paleomagnetic data for the Devonian rocks in the Western Mongolia-Okhotsk Foldbelt, *Geol. Pacific Ocean, 16,* 1107–1123.

Li, Y. P., M. O. McWilliams, H. Zhu, et al. (1985), Paleozoic paleomagnetic results from the Hexizoulang Terrane, China, *EOS Trans. AGU, 66,* 864.

Lin, J. L., M. Fuller, and W. Y. Zhang (1985), Preliminary Phanerozoic polar wander paths for the North and South China blocks, *Nature, 313,* 444–449.

Lowrie, W. (1990), Identification of ferromagnetic minerals in a rock by coercitivity and unblocking temperature properties, *Geophys. Res. Lett., 17*(2), 159–162.

Ma Xing-hua, Xing Li-sheng, and Yang Zyth-yu (1993), Paleomagnetic study since Late Paleozoic in the Ordos Basin, *Acta Geophysica Sinica, 36*(1), 68–79.

McElhinny, M. W. (1964), Statistical significance of the fold test in paleomagnetism, *Geophys. J. R. Astron. Soc., 8,* 338–340.

McFadden, P. L. (1990), A new fold test for paleomagnetic studies, *Geophys. J. Int., 103,* 163–169.

McFadden, P. L., and D. L. Jones (1981), The fold test in paleomagnetism, *Geophys. J. R. Astron. Soc., 67,* 53–58.

McFadden, P. L., and M. W. McElhinny (1988), The combined analysis of remagnetization and direct observation in paleomagnetism, *Earth Planet. Sci. Lett., 87,* 161–172.

McFadden, P. L., and M. W. McElhinny (1990), Classification of the reversal test in paleomagnetism, *Geophys. J. Int., 103,* 725–729.

Meng, Z. F., and R. S. Coe (1992), The Late Silurian paleomagnetic results for the Hexi Corridor and its tectonic implication, *Sci. China, 22*(ser. B), 531–536.

Nagata, T. (1965), *Rock Magnetism,* pp. 346, Translated by MIR Publishers, Moscow.

Nagibina, M. S. (1963), Tectonics and Magmatism of the Mongolia-Okhotsk Belt, *Proc. Geol. Inst.,* Iss. 79, 463 pp.

Natal'in, B. A. (1991), Mesozoic accretion and collision tectonics of the Far East region of the USSR, *Pacific Geology,* (5), 3–23.

Otofuji Yo-ichiro, K. Kasuragi, et al. (1989), Remagnetization of Cambrian to Triassic sedimentary rocks of the Paegunsan syncline in the Okchon zone, South Korea, *J. Geomagn. Geoelectr., 41,* 119–135.

Otofuji Yo-ichiro, T. Matsuda, T. Itaya, et al. (1995), Late Cretaceous to Early Paleogene paleomagnetic results from Sikhote-Alin, Far-Eastern Russia: Implications for the deformation of East Asia, *Earth Planet. Sci. Lett.,* (130), 95–108.

Parfenov, L. M., A. N. Bulgatov, and I. V. Gordienko (1996), Terrains and orogenic belts in the East Baikal region, *Pacific Geology, 15*(4), 3–15.

Parfenov, L. M., L. I. Popeko, and O. Tomurtogoo (1999), Problems of tectonics of Mongolia-Okhotsk orogenic belt, *Pacific Geology, 18*(4), 24–43.

Pecherskii, D. M., and A. N. Didenko (1995), *Paleoasian Ocean: Petromagnetic and Paleomagnetic Information for Its Lithosphere,* 297 pp., OIFZ RAN, Moscow.

Pruner, P. (1987), Paleomagnetism and paleogeography of Mongolia in the Cretaceous, Permian, and Carboniferous: Preliminary data, *Tectonophysics, 139,* 155–167.

Raposo, M. I. B., M. S. D'Agrella-Filho, R. Siqueira (2003), The effect of magnetic anisotropy on paleomagnetic directions in high-grade metamorphic rocks from the Juiz de Fijra Complex, SE Brazil, *Earth Planet. Sci. Lett., 209,* 131–147.

Shipunov, S. V. (1995a), A new fold test in paleomagnetism: Rehabilitation of the alignment test, *Physics of the Earth,* (4), 67–74.

Shipunov, S. V. (1995b), Synfolding magnetization: Estimation of its trend and geological application, *Physics of the Earth,* (11), 40–47.

Shipunov, S. V., and Yu. S. Bretshtein (1999), Problems of component analysis in paleomagnetism, *Physics of the Earth,* (3), 52–61.

Shipunov, S. V., and A. A. Muraviev (2000), The sensitivity and reliability of a fold test in paleomagnetism, *Physics of the Earth,* (7), 10–16.

Tan, X., and K. P. Kodama (2002), Magnetic anisotropy and paleomagnetic inclination shallowing in red beds: Evidence from the Mississippian Mauch Chunk Formation, Pennsylvania, *J. Geophys. Res., 107*(B11), 2311, doi:10.1029/2001JB001636.

Ustritskii, B. I., and A. N. Khramov (1987), The formation history of the Northern Pacific Ocean and the Pacific mobile belt, in *Essays on the Geology of the Northwestern Segment of the Pacific Tectonic Belt,* pp. 239–276, Nauka, Moscow.

Wang, Z., and R. Van der Voo (1993), Pervasive remagnetization of Paleozoic rocks acquired at the time of Mesozoic folding in the South China Block, *J. Geophys. Res., 98*(B2), 1729–1741.

Watson, G. S., and R. J. Enkin (1993), The fold test in paleomagnetism as a parameter estimation problem, *Geophys. Res. Lett., 20,* 2135–2137.

Wu, H. N., L. F. Zhou, Z. Y. Zhao, and Y. Chen (1993), Tectonic implications of the paleomagnetic results for the late Paleozoic and Mesozoic rocks from the Ala-Shan area of the western north of the China block, *Sci. Geol. Sin.,* (2), 19–46.

Yang, C., and V. Courtillot (1989), Widespread Cenozoic (?) remagnetization in Thailand and its implications for the India-Asia collision, *Earth Planet. Sci. Lett.,* (93), 113–122.

Yang, Z., X. Ma, J. Besse, et al. (1991), Paleomagnetic results from Triassic sections in the Ordos Basin, North China, *Earth Planet. Sci. Lett.,* (104), 258–277.

Yang, Z., V. Courtillot, J. Besse, et al. (1992), Jurassic paleomagnetic constraints for the collision of the North and South China Blocks, *Geophys. Res. Lett., 19*(6), 577–580.

Yang, Z., Y. Otofuji, Z. Sun, and B. Huang (2002), Magnetostratigraphic constraints on the Gondwanan origin of North China: Cambrian/Ordovician boundary results, *Geophys. J. Int.,* (151), 1–10.

Zakharov, Yu. D., and A. N. Sokarev (1991), Biostratigraphy and Paleomagnetism of Permian and Triassic Rocks in Eurasia, 135 pp., Nauka, Moscow.

Zhao, X., R. Coe, C. Liu, and Y. Zhou (1992), New Cambrian and Ordovician paleomagnetic poles for the North China Block and their paleogeographic implications, *J. Geophys. Res., 97*(B2), 1767–1788.

Zhao, X., R. Coe, H. Wu, and Z. Zhao (1993), Silurian and Devonian paleomagnetic poles from North China and implications for Gondwana, *Earth Planet. Sci. Lett., 117,* 497–506.

Zhao, X., R. Coe, S. A. Gilder, and G. M. Frost (1996), Paleomagnetic constraints on the paleogeography of China and implications for Gondwanaland, *Aust. J. Earth Sci., 43,* 643–672.

Zhenyu, V., Otofuji Yo-ichiro, H. Baochun, and S. Zhiming (1999), Paleomagnetic evidence for the affinity of with Gondwana, *Geol. Reviews, 45*(4), 402–407.

Zhu, H., and Z. X. He (1987), An attempt of the paleomagnetic and tectonic study of Paleozoic strata from the northern margin of the Alashan terrane, in *Biostratigraphy and Tectonics of Paleozoic Strata Along the Alashan Terrane Margin,* pp. 154–159, Wuhan Geological College Press, Wuhan.

Zijderveld, J. D. A. (1967), A.C. demagnetization of rocks: Analysis of results, in *Methods in Paleomagnetism,* edited by D. W. Collinson and K. M. Kreer, pp. 254–286, Elsevier Publ. Co., Amsterdam.

Zonenshain, L. P., M. I. Kuzmin, and L. M. Natapov (1990), *Plate Tectonics of the USSR Territory,* Book 1, 328 pp., Book 2, 336 pp., Nedra, Moscow.

Yu. S. Bretshtein and A. V. Klimova, Institute of Tectonics and Geophysics, Far East Division, Russian Academy of Sciences, e-mail: bret@itig.as.khb.ru

(Received 27 October 2004)